Measurement of Partial Conversions During the Solution Copolymerization of Styrene and Butyl Acrylate Using On-Line Raman Spectroscopy

MARK VAN DEN BRINK,[1] JACQUES-FRANÇOIS HANSEN,[1] PETER DE PEINDER,[2] ALEX M. VAN HERK,[1] ANTON L. GERMAN[1]

[1] Department of Polymer Chemistry and Coating Technology, Eindhoven University of Technology, PO Box 513, 5600 MB Eindhoven, The Netherlands

[2] Department of Analytical Molecular Spectroscopy, Utrecht University, Sorbonnelaan 16, 3584 CA Utrecht, The Netherlands

Received 15 October 1999; accepted 14 March 2000

ABSTRACT: The copolymerization of styrene and *n*-butyl acrylate in dioxane was monitored by on-line Raman spectroscopy. The calculation of the individual monomer concentrations on the basis of the individual vinyl peaks is not straightforward for this system, as these bands are overlapping in the Raman spectrum. To tackle this problem, univariate and multivariate approaches were followed to obtain monomer concentrations and the results were validated by reference gas chromatography data. In the univariate analysis, linear relations between various monomer peaks were used to calculate monomer concentrations from the Raman data. In principal component analysis, the main variation in the spectra could be ascribed to conversion of monomer. Furthermore, principal component analysis pointed out that the second-largest effect in the spectra could be attributed to experiment-to-experiment variation, probably attributable to instrumental factors. In the multivariate partial least squares regression approach, single factor models were used to calculate monomer concentrations. Both the univariate and the partial least squares regression approaches proved successful in calculating the individual monomer concentrations, showing very good agreement with off-line gas chromatography data. © 2000 John Wiley & Sons, Inc. J Appl Polym Sci 79: 426–436, 2001

Key words: copolymerization; on-line Raman spectroscopy; multivariate analysis

INTRODUCTION

In copolymerization processes, the final product properties of the copolymer strongly depend on the chemical composition distribution.[1] The composition of the instantaneously formed copolymer, in turn, depends on the comonomer concentration, and this relation is usually well described by the ultimate copolymerization model.[2] As a consequence, controlling copolymer composition can be achieved by controlling the comonomer composition. Hence, information on comonomer concentration is of major importance, and this can be achieved in several ways: 1. by measuring all monomer concentrations directly by, e.g., gas chromatography (GC)[3] or spectroscopic techniques[4,5]; 2. by measuring the overall conversion

Correspondence to: A. L. German.

Contract grant sponsors: Foundation Emulsion Polymerization (SEP) and Priority Program Materials (PPM-NWO).

Journal of Applied Polymer Science, Vol. 79, 426–436 (2001)

by, e.g., densitometry,[6] ultrasound methods,[7] or calorimetry[8] in conjunction with a model such as the Mayo-Lewis equation[2] to calculate the composition of the comonomer mixture; and 3. by open-loop strategies,[9] in which control is based on a theoretical model without monitoring the reaction.

Disadvantages of using the latter two techniques is that these methods are model dependent and, in addition, the third approach is insensitive to disturbances of the process by, e.g., contamination of the reactor by inhibiting species such as oxygen, or inaccuracy of the feed pumps.

A promising method for monitoring monomer concentrations is Raman spectroscopy. The technique has been applied in bulk,[10] solution,[11] emulsion,[12–18] and suspension[19] polymerizations. The technique is especially promising for emulsion and suspension polymerizations because transparency is not required because Raman spectroscopy is a scattering technique. Furthermore, water is only a weak scatterer, not obscuring the spectrum. In addition, the application of fiber optics[13,14] is readily possible because light in the visible or near infrared light region can be used, offering opportunities for remote, *in situ* monitoring.[20]

In the literature, a few studies have been reported in which Raman spectroscopy is used for determining monomer concentrations in copolymerizations.[21–23] Bowley et al.[21] studied the copolymerization of styrene and methyl methacrylate and applied Fourier self-deconvolution to obtain the relative vinyl bands. They claimed that this approach was successful, although they did not give any details or show validation of the results.

Haigh et al.[22] studied the copolymerization of styrene with vinyl imidazole to estimate reactivity ratios. The emulsion copolymerization of styrene and butyl acrylate has previously been studied by Raman spectroscopy by Al-Khanbashi et al.[23] In this study, a univariate approach was used to calculate monomer concentrations.

The goal of the present report is to compare the accuracy of univariate and multivariate techniques, focusing on the calculation of the individual monomer concentrations of butyl acrylate and styrene. Because Raman spectroscopy is a scattering technique, concentrations cannot be calculated from absolute intensities because of variations in, e.g., optical alignment or sampling volume, and spectra need to be normalized.[24] For this reason, we have chosen to work with solution polymerizations. The advantage of studying solution polymerizations is that a solvent peak can be used as an internal standard. In this way, the problems related to normalization of the spectra or assuming constant monomer bands are avoided.

Styrene and butyl acrylate have vinyl bands with Raman shifts of 1631 cm^{-1} and 1635 cm^{-1}, respectively.[25,26] As a result, the individual monomer peaks are strongly overlapping and the area of the resulting vinyl peak cannot be related to individual monomer concentrations. In the multivariate approach,[27] the full spectrum can be used, and changes in the spectrum are correlated to changes in monomer concentrations. Therefore, a calibration set is required to predict monomer concentrations in unknown samples. For this reason, off-line samples were taken and analyzed by GC.

In the univariate approach, results from the homopolymerizations are used to calculate monomer concentrations from the copolymerization Raman data, by using relations between various bands in the Raman spectrum.

EXPERIMENTAL

Materials

The monomers, styrene (Sty, >99%; Merck, The Netherlands) and butyl acrylate (BA, >99%; Merck) were purified from inhibitor (*t*-butylcatechol and hydroquinone, respectively) by passing them over an inhibitor-removing column (Dehibit 200; PolySciences). Dioxane (Merck, p.a.) and α-α'-azobis-isobutyronitrile (AIBN; Fluka, The Netherlands) were used as received.

Setup

Raman spectra were recorded with a Labram spectrometer (Dilor S.A., France). A Spectra Physics Millenium II Nd:YVO_4 laser, operated at 532 nm, was used as an excitation source. The initial laser power was 0.40 W, which resulted in approximately 0.15 W at the sample. Spectra were taken *in situ* from a 0.3-L glass reactor with a heating jacket for controlling temperature. Raman spectra were acquired through a single wall glass window. The optical head (Superhead, Dilor S.A.) was placed in front of this window and was connected to the spectrometer using 10 m of optical fiber, as shown in Figure 1. The spectrometer was equipped with an 1800 grooves/mm grating

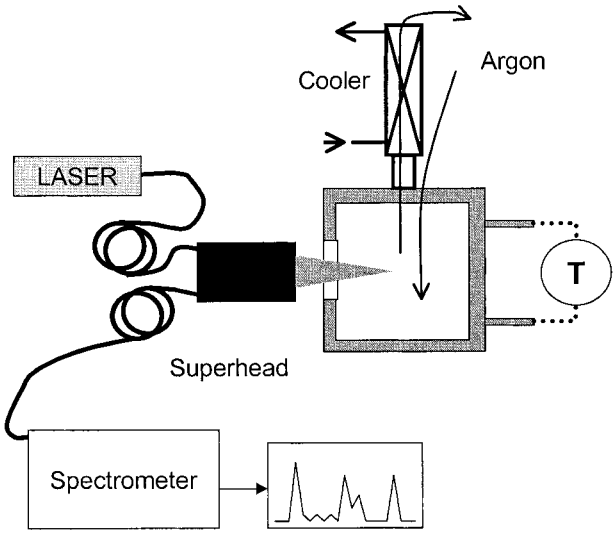

Figure 1 Schematic set-up of the on-line Raman equipment.

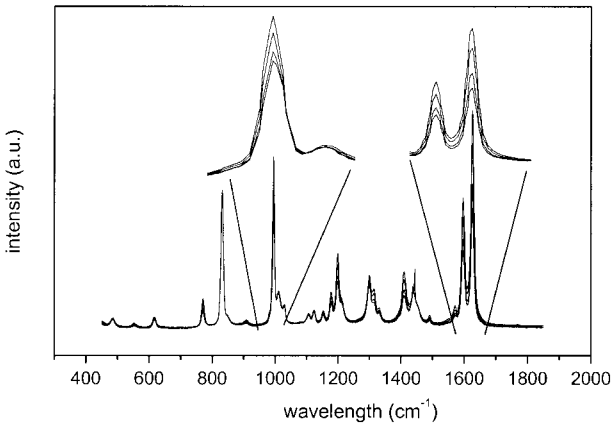

Figure 2 Some smoothed, normalized spectra from the homopolymerization of styrene at 0, 20, 40, and 60% conversion.

and a charge-coupled device, resulting in a resolution of 0.045 nm (approximately 1.5 cm^{-1}).

Off-line samples (approximately 1 mL) were diluted in tetrahydrofurane and analyzed by GC. The HP 5890 gas chromatograph was equipped with an autosampler and Alltech AT-wax column (length, 30 m; film thickness, 1.0 μm). Table I gives the recipes for the various reactions and conditions for the measurements. Polymerizations were performed under an argon atmosphere by maintaining a mild argon flow (<2 mL/min) at 60°C, while the reaction medium was mixed using a magnetic stirrer.

Before analyzing the Raman data, spectra were subsequently smoothed, baseline corrected, and normalized. Smoothing was performed by applying a seven-points Savitsky-Golay filter twice. The spectra were baseline corrected either by a polynomial spline for the complete spectrum, or by linear interpolation for small regions. The normalization was accomplished by dividing the individual intensities after smoothing and baseline correction by the integrated area of the ring-breathing band of dioxane[28] from 800–880 cm^{-1}.

Principal component analysis (PCA) and partial least squares regression (PLSR) were performed using commercial software (The Unscrambler 6, Camo A.S., Norway).

RESULTS AND DISCUSSION

Homopolymerizations

Figures 2 and 3 show some spectra which were obtained during the polymerizations of Sty and BA (HSty and HBA), respectively. Both Figures show that, during polymerization, the solvent peaks remain constant (e.g., peaks at 830, 1030, and 1430 cm^{-1}), whereas the intensity of the monomer peaks decrease during polymerization. In Figure 2, for example, the aromatic peaks at 1600 and 1000 cm^{-1} decrease with increasing conversion. In Figure 3, the peak with most pronounced decrease besides the vinyl peak in the

Table I Recipes for the Various Reactions

Reaction	Initiator (g)	Styrene (g)	BA (g)	Dioxane (g)	t_{acq} (s)	Alternative Technique
C1	0.23	37.43	87.42	132.00	60	GC
C2	2.05	37.93	88.36	131.92	60	GC
C3	1.65	37.60	87.71	132.112	60	GC
HSty	0.99	59.52	0	187.91	60	Grav.
HBA	0.22	0	99.10	151.52	15	Grav.

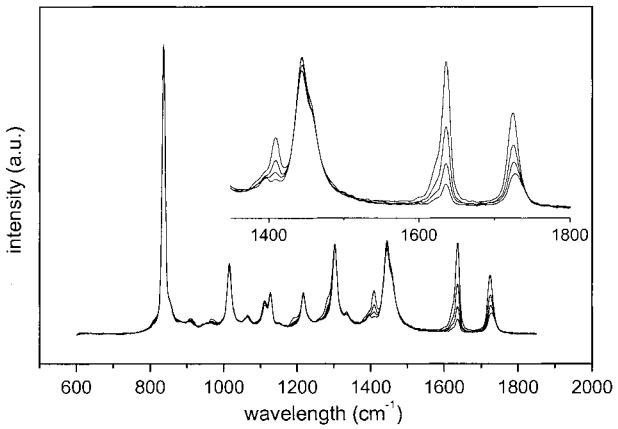

Figure 3 Some smoothed, normalized spectra from the homopolymerization of BA (HBA) at 0, 50, 70, and 85% conversion.

polymerization of BA, is the carbonyl band near 1730 cm^{-1}. It has previously been shown that for the polymerization of methyl methacrylate, the carbonyl band can be used for monitoring conversion.[11]

Figure 4 shows that the intensities of the aromatic and carbonyl bands mentioned above decrease linearly with increasing conversion. In this Figure, conversion is calculated according to the normalized area of the decreasing vinyl band. Using these linear relations, it is possible to calculate conversion according to eq. (1):

$$X(i) = \frac{1 - \dfrac{A(i)}{A(0)}}{K} \tag{1}$$

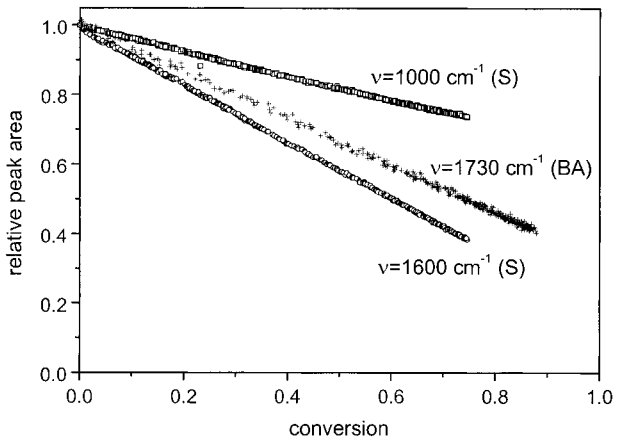

Figure 4 Relative peak areas [$A(i)/A(0)$] as a function of conversion for the solution polymerizations of Sty and BA.

Table II *K* Values Obtained from the Solution Polymerizations of Styrene and Butyl Acrylate

Monomer	Region (cm^{-1})	*K*
Styrene	990–1010	0.3518
Styrene	1600	0.8513
Butyl acrylate	1680–1760	0.6725

where $X(i)$ stands for the conversion corresponding to spectrum i, $A(i)/A(0)$ for the relative area (or intensity) of the peak of interest for spectrum i relative to the initial area, whereas K is obtained from the linear fit (in all cases $R^2 > 0.999$). Table II shows some values for K obtained from polymerizations B1 and B2.

The results obtained in this study contrast with those from a previous study on the system of styrene and butyl acrylate by Al-Khanbashi et al.[23] In their study, it was assumed that the aromatic ring-breathing band for styrene at 1000 cm^{-1} remained constant during polymerization. Next, they calculated the styrene conversion using the olefinic CH deformation band at 1412 cm^{-1} (see Fig. 2), assuming no contribution from BA in this region. The BA concentration was subsequently calculated from the BA vinyl area, which was obtained by subtracting the estimated styrene vinyl area, calculated from the styrene conversion data, from the total vinyl area.

Our results, however, indicate that the intensity of the aromatic ring-breathing mode decreases with conversion, as shown in Figures 2 and 4. The same decrease was previously observed during the bulk polymerization of styrene.[25] Therefore, the assumption that the ring-breathing mode remains constant,[23] seems incorrect. Furthermore, Figure 3 shows that BA also displays a peak near 1412 cm^{-1}, disappearing with increasing conversion, implying that during the copolymerization of Sty and BA, the peak at 1412 cm^{-1} cannot be ascribed to Sty alone.

Copolymerizations

Figure 5 shows the amounts of monomer in the reactor versus time, whereas Figure 6 shows the monomer fraction versus conversion for the monomer concentrations as obtained by GC. The difference in conversion-time behavior (see Fig. 5) can be accounted for by the varying initiator concentrations. However, Figure 6 shows that the three copolymerizations are identical, because all

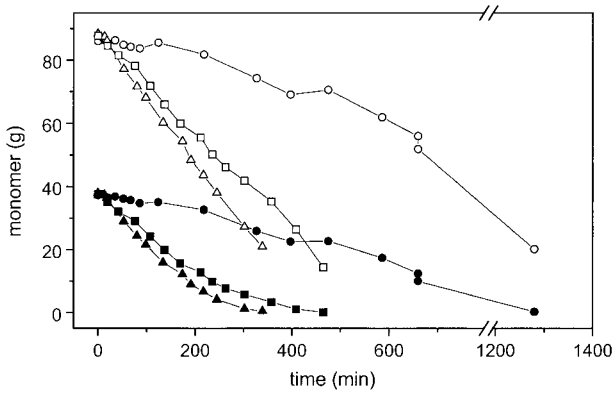

Figure 5 Styrene (filled symbols) and butyl acrylate (open symbols) as a function of time. ○, C1; △, C2; □, C3.

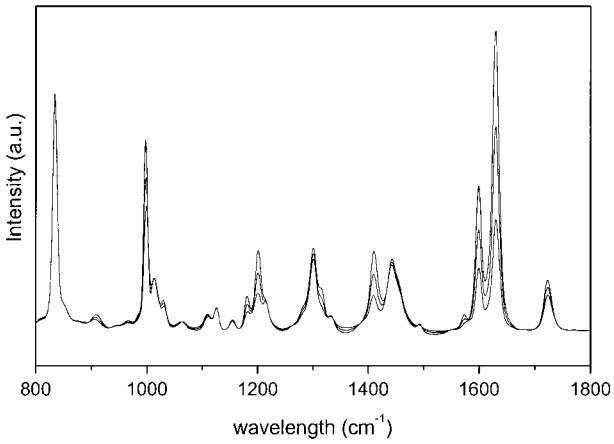

Figure 7 Some smoothed, normalized spectra from the copolymerization of Sty and BA (C2).

GC data are well fitted,[29] using only one pair of reactivity ratios (r_{Sty} = 0.80 and r_{BA} = 0.23). In other words, reactions C1–C3 are going through the same states in terms of composition, although the time at which a certain state is reached differs from reaction to reaction.

Figure 7 shows some of the spectra obtained during copolymerization reaction C2 and similar spectra were obtained from reactions C1 and C3. The Figure shows that, although these are lower concentrations of Sty compared with BA, spectra are dominated by Sty and the solvent.

Univariate Analysis

The values for K as presented in Table II can be used to estimate partial conversions and from these the monomer concentrations. These monomer concentrations can then be compared with the GC results. This comparison is shown in Figure 8, displaying the amounts of BA and Sty versus time for reaction C2. It can be seen that the GC and Raman results are in good agreement. Figure 9 compares the results of the Raman data with the corresponding GC data for reactions C1–C3, where "measured" refers to the monomer concentrations measured by GC and "predicted" to the monomer concentrations calculated from the Raman data. Figures 8 and 9 clearly demonstrate that, using the univariate approach, monomer concentrations can be calculated successfully.

Multivariate Analysis

PCA

PCA was performed on the spectra from C1–C3 for which the monomer concentrations were ana-

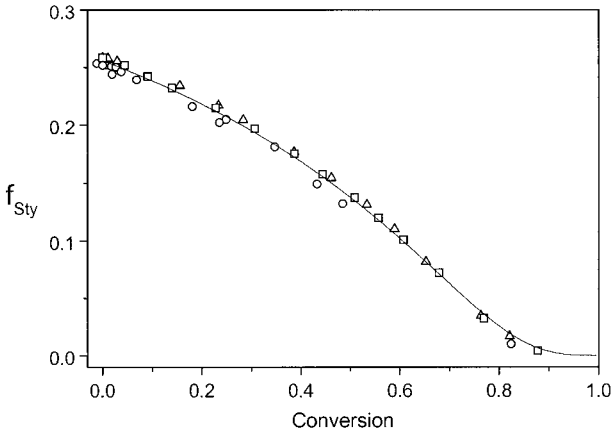

Figure 6 Conversion versus monomer fraction. ○, C1; △, C2; □, C3, _____, model prediction (r_{Sty} = 0.8, r_{BA} = 0.23).

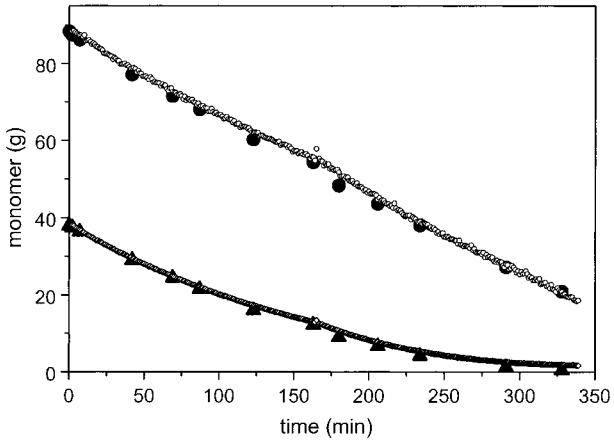

Figure 8 Monomer content as a function of time. ○, BA; △, Sty. Open symbols, Raman data; closed symbols, GC data.

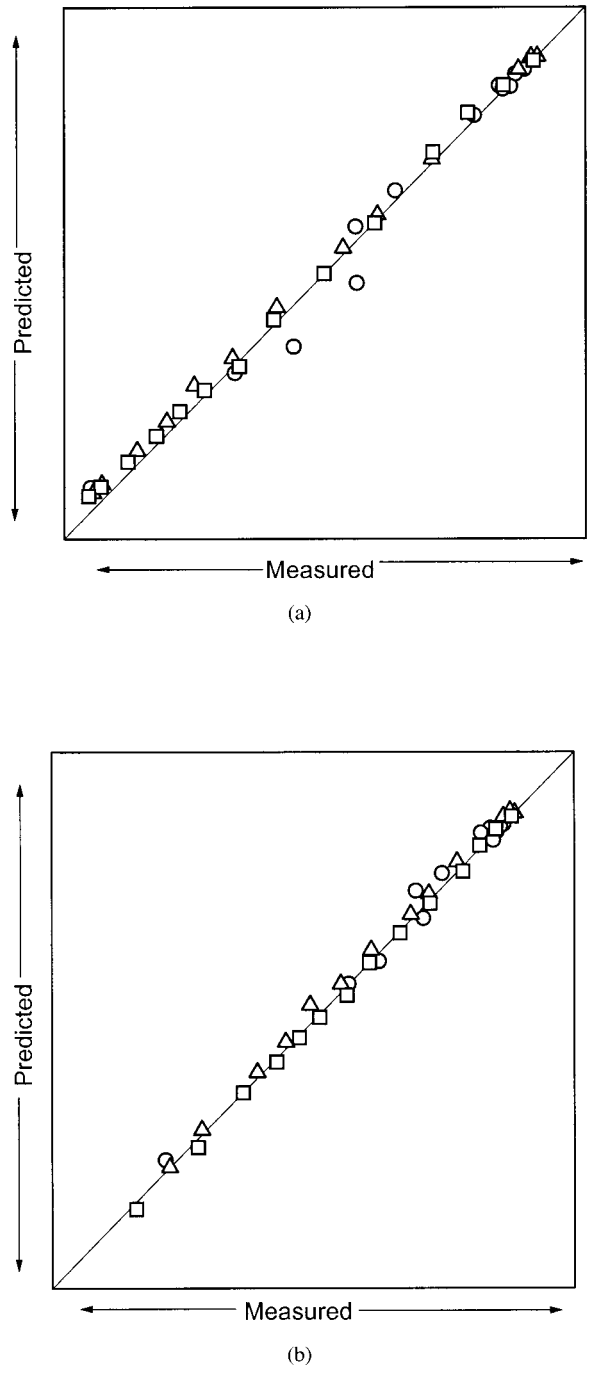

Figure 9 (a) Predicted versus measured styrene concentrations for univariate analysis. ○, C1; △, C2; □, C3. (b) Predicted versus measured butyl acrylate concentrations for univariate analysis. ○, C1; △, C2; □, C3.

lyzed using GC. PCA is a powerful mathematical technique for studying spectral variations in a data set. In PCA, the spectrum is decomposed in scores and loading vectors, according to:

$$\mathbf{x} = t_1 \cdot \mathbf{p}_1 + t_2 \cdot \mathbf{p}_2 + \cdots + t_n \cdot \mathbf{p}_n = [t_1 \ldots t_n] \times \begin{bmatrix} \mathbf{p}_1 \\ \vdots \\ \mathbf{p}_n \end{bmatrix} = \mathbf{t}^T\mathbf{P} \quad (2)$$

where $\mathbf{x}$ represents the spectrum, $\mathbf{p_1}$ the first loading vector, and t_1 the score belonging to the first loading vector. The maximum number of components possible, n, equals the number of spectra in the complete set. However, usually most of the spectral variation is described by the first few components, whereas the higher loading vectors represent mainly noise in the spectra. To study the variation in the spectral set, only the first loading vectors and the accompanying scores need to be taken into account. The loading vectors, also called principal components (PCs), can be regarded as the "building blocks" and the scores as "the number of building blocks" needed to reconstruct a spectrum. Thus, the same "building blocks" are used for all the spectra in the set, whereas the number of blocks varies from spectrum to spectrum or, associated to the spectra, from sample to sample. Therefore, within a set, a sample is characterized by its scores, whereas the set as a whole is characterized by its loading vectors. PCA is described in great detail in Martens and Næs.[27]

Before PCA, all spectra were smoothed, normalized, and baseline corrected as described in the previous section. In addition, spectra were mean-centered by subtraction of the average spectrum, calculated from the complete data set. In this way, the results are interpreted as variations around the mean. PCA was performed on all Raman spectra for which a corresponding GC sample was taken, giving a total of 37 spectra in the set. Figure 10 shows the explained variance versus the number of PCs. The explained variance indicated here as a percentage, is a measure of the proportion of variation in the data accounted for by the current PC. Figure 10 shows that by using 1 PC, 98% of the spectral variation is accounted for, whereas two PCs account for 99.5% of the spectral variation. Figure 11, depicting loading vectors 1 to 5, also shows that the noise in the loading vectors increases with increasing number of components.

In addition, Figure 11 shows that the peaks for styrene are most prominently present in the first loading, whereas BA is only visible in this loading by the small peak in the area of the carbonyl peak (1730 cm^{-1}). Furthermore, in the first loading,

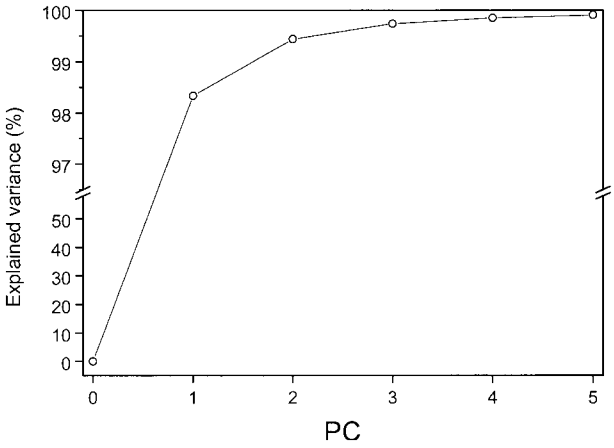

Figure 10 Explained variance as a function of the number of components for PCA on the full spectrum for C1–C3.

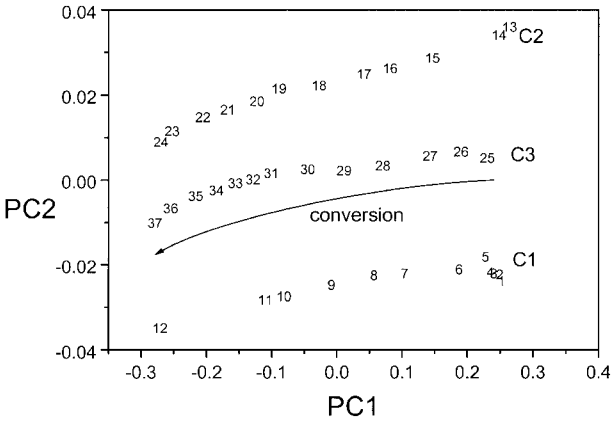

Figure 12 Scoreplot for the complete calibration set resulting from PCA on the full spectrum (450–1850 cm^{-1}).

the solvent peaks are virtually absent, although they are clearly present in the spectra (cf. Fig. 8). In the second loading, the most prominent peak coincides with the solvent band near 830 cm^{-1}. Looking more closely at Figure 11, it seems that the second loading is a "derivative" of the original spectrum. The derivative-like appearance of a loading often indicates a peak shift, rather than an effect in composition. This effect may be caused by a variation from experiment to experiment. The scoreplot corroborates this supposition. Figure 12 shows the scores along PC2 versus the scores along PC1 for the samples in the set. The numbers denote the sample number, 1–12 for C1, 13–24 for C2, and 25–37 for C3, the numbers increasing with conversion. It seems that PC1 is mainly related to conversion; with increasing conversion, the scores on PC1 decreases, whereas the main variation in PC2 seems to be the experiment from which the sample is taken, rather than the small effect which seems to be caused by conversion.

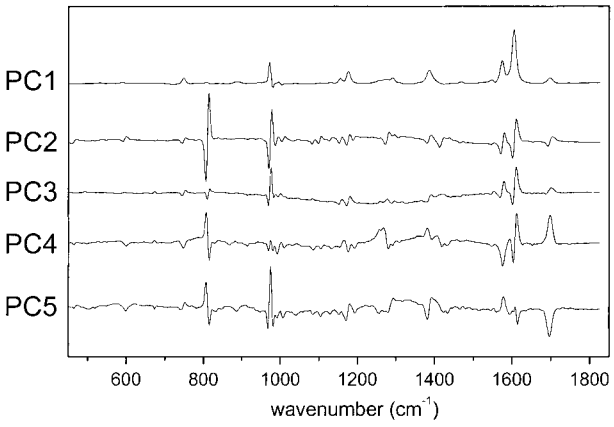

Figure 11 First five loadings for the PCA on C1–C3 for the full spectrum.

The origin of this variation may be in instrumental (hardware) factors, or attributable to pretreatment of the spectra (software factors). However, all spectra were treated using the same Savitsky-Golay filter and the same baseline correction. Taking derivatives instead of a baseline correction did not markedly change the score plots. Also, PCA was performed on spectra that were not normalized. In this case, a higher factor model was required to describe the variation in the data and the experiment-to-experiment variation being also present in the first factor (not shown). Thus, software factors seem unlikely to account for the variation.

Instrumental variance does not seem unreasonable, as the alignment of the spectrometer changes from experiment to experiment. The spectrometer is equipped with an adjustable grating, which may be the origin of the shifts. In calibrating the system, the grating is turned to a different position, and later turned back to approximately the same position as in previous experiments. However, we have found that it is virtually impossible to turn the grating back to exactly the same position, and variations (shifts) of around 1 cm^{-1} are encountered. In addition, small variations in the laser frequency may give the same effect. However, in calibrating the system, the laser frequency is taken as 0 cm^{-1} Raman shift and a distinction between these two

Table III Results for Calibration Models (PLSR)

	Sample Set	Region (cm^{-1})	Assignment	#PC (Sty)	σ_p (Sty) $\times 10^3$	#PC (BA)	σ_p (BA) $\times 10^3$
1	All	450–1850	Full spectrum	1	8.12	3	1.43
2	C1	450–1850	Full spectrum	1	12.1	3	26.2
3	C2	450–1850	Full spectrum	1	3.49	2	3.44
4	C3	450–1850	Full spectrum	1	2.69	2	4.53
5	C3	1690–1760	C═O	1	23.2	1	4.82
6	C3	1550–1680	C═C	1	2.81	2	4.71
7	C3	1390–1530	═CH	1	4.09	3	6.69
8	C3	1140–1370	—CH	1	2.97	2	8.609
9	C3	930–1040	Aromatic	1	2.96	3	21.0
10	C3	450–880		1	3.05	2	14.9

#PC, number of factors used in the model; σ_p, root mean squared error of prediction.

effects is difficult. Reactions C2 and C3 have been performed on subsequent days, whereas reaction C1 was performed 4 weeks earlier. As a consequence, between reactions C1 and C2, the grating was repositioned, whereas it was not between C2 and C3. In between all reactions, the laser was shut off and on again. These operations may be the cause of experiment-to-experiment variation.

The conclusion is that, in the spectra, the main variation is given by converting monomer to polymer, and a second effect is present because of experiment-to-experiment variation, which cannot be ascribed to the reaction itself. This second effect is smaller than the first, though clearly present in the PCA. Adaptive calibration models[30] may be able to correct for these small peak shifts. The observation that only one factor describes variations attributed to polymerization coincides with the linear relationships between the vinyl and other bands.

PLSR

PLSR resembles PCA. The main difference is that PLSR is a regression technique, requiring a calibration step and therefore calibration samples, whereas PCA does not require this. As in PCA, in PLSR, spectra are "reconstructed," similar to eq. (2). In PLSR, in contrast with PCA, the loading vectors and scores are determined by regressing the variation in the spectra to the variation in the samples. A detailed description of PLSR can be found in the literature.[27]

As in any calibration, the samples in the calibration set should represent the full range of conditions encountered during the reaction. As discussed previously, reactions C1–C3 are identical, and for this reason each of these reactions can serve as the calibration set for calculating concentrations obtained from the other reaction.

PLSR Calibration

PLSR was performed on various parts of the spectrum, for both Sty and BA, for all samples (C1–C3) and the individual sets. Table III shows the results for the various calibration models that were constructed. The calibration models were validated by a full cross validation.[27] The quality of the models is expressed by σ_p, the root mean squared error of prediction, given by the weighted squared residual between the predicted concentration by the model and the concentration as measured by GC.[31] A low value for σ_p indicates a high accuracy in the prediction of the monomer concentration and is expressed in grams of monomer per gram of solvent.

Table III shows that, in all cases, the styrene concentration is predicted using single factor models. This is probably because variations in the spectrum are dominated by styrene. Oddly, even the carbonyl area results in a single factor model for styrene, although this monomer shows no bands in this region. However, the high value for σ_p indicates that the prediction is not very accurate and indeed there is a significant difference between the measured and predicted values. The fact that a prediction can still be made is due to the co-linearity in the BA and Sty concentrations; a decreasing concentration of one monomer is always accompanied by a decrease in the other, whereas the difference between the actual and calculated data describes the deviation from lin-

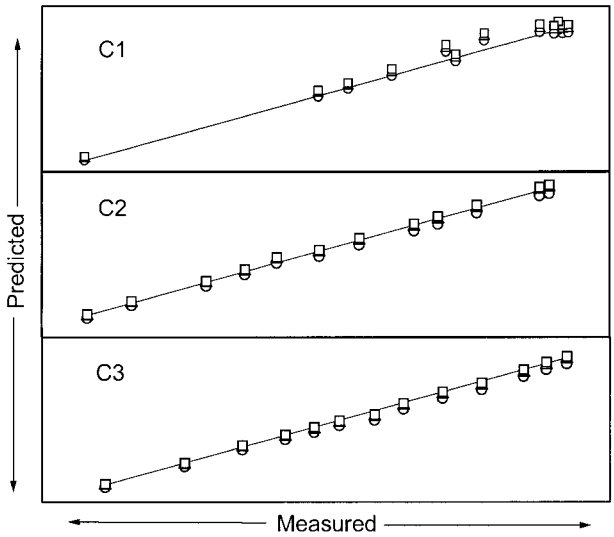

Figure 13 Measured concentrations versus the predicted concentrations for BA. _____, exact match; ○, C1 for calibration; △, C2 for calibration; □, C3 for calibration.

ear behavior in the decreasing comonomer concentrations.

For BA, two to three factor calibration models are required, except for the carbonyl area in which a single factor suffices. The two to three factor models are, again, probably due to the co-linearity in the Sty and BA concentration. The first factor gives the main variation due to styrene, whereas higher factors describe the deviation from linearity. Note that, in regions where much more Sty is present than BA, the number of factors is at least two, whereas if BA is virtually absent (e.g., the aromatic region around 1000 cm^{-1}), a three-factor model is required. In the case of the carbonyl region (around 1730 cm^{-1}), a single factor gives good predictions, as in this case no co-linearity resulting from the styrene can be expected.

PLSR Prediction

Using the calibration models from the previous section, concentrations for Sty and BA for one reaction can be calculated using the calibration model from another; i.e., concentrations from C1 can be calculated using the calibration models constructed from reaction C2 and/or C3, and vice versa. The BA concentrations were calculated using calibration models based on the carbonyl area for sets C1–C3 (cf. set 5, Table III). The results are shown in Figure 13 where the results for C1, C2, and C3 are shown as predicted versus measured plots. The line represents the "ideal case," where the predicted (Raman) values equal the measured (GC) values. It can be seen that in all cases, accurate predictions are obtained. This is also shown in Table IV, giving the standard deviations in the BA concentrations (σ_{BA}). Table IV and Figure 13 show that, when C1 is used in the calibration model, a lower precision in the results is obtained. This is probably because of the lower precision from the GC results. C2 and C3 show approximately the same precision.

Obviously, the best predictions are obtained when calculating concentrations within calibration set.

The results shown for the predictions are only for BA. The results for Sty gave lower values for σ_{Sty}, compared with σ_{BA}, indicating higher precision. This was expected because of the values for σ_p for calibration sets 6, 8, or 9 in Table III.

Table IV Standard Deviations σ_{BA} for BA for the Individual Data Sets (Columns) for Different Calibration Sets (Rows)

Prediction →	C1	C2	C3
Calibration ↓	σ_{BA} ($\times 10^3$)	σ_{BA} ($\times 10^3$)	σ_{BA} ($\times 10^3$)
C1	9.02	41.4	22.9
C2	22.1	2.25	8.2
C3	16.2	11.9	3.23

Calibration is performed by PLS1 on the CO peak (1680–1760 cm^{-1}).

Univariate Predictions Versus Multivariate Predictions

Comparing the univariate and PLSR predictions for BA in Figures 9(b) and 13, and Tables IV and V, it can be seen that the PLSR results yield a little higher precision. However, the quality of the

Table V Standard Deviations Using Reaction B2 for Calibration

	Univariate ($\sigma_{BA} \times 10^3$)	PLSR ($\sigma_{BA} \times 10^3$)
C1	17.5	29.6
C2	13.7	37.9
C3	6.7	26.3

σ_{BA} expressed in g monomer/g solvent.

PLSR predictions depends strongly on the quality of the calibration model, which hampers the robustness of this technique. In the case presented herein, the accuracy of PLSR seems to be limited by instrumental factors. Whether this limitation in precision is disturbing depends on the constraints of, e.g., a controller model. Furthermore, it should be noted that the sets C1–C3 are very similar. Greater variation between the prediction and calibration may decrease accuracy. Therefore, the PLSR results presented herein can be regarded as almost "ideal," given that instrumental variation cannot be avoided and variations in experimental conditions can only increase.

The univariate prediction, on the other hand, seems more robust in this respect, because the requirements for the calibration set are less strict. Additionally, as integrated peak areas are used, this approach seems less sensitive to instrumental variation.

As briefly mentioned previously, in the comparison of the univariate method and the multivariate approach, different sets were used for calibration. To use the homopolymerization of BA for a multivariate prediction, a PLSR model was developed, which is able to predict (partial) conversions of BA. From the partial conversions and the initial concentration of BA, the actual concentrations of BA can be calculated. The results of these PLSR predictions can be compared with univariate predictions using the same calibration set. To do so, spectra for both the homo- and copolymerization in the carbonyl region of 1690 to 1760 cm^{-1} were scaled to the spectrum at zero conversion, according to the following equation:

$$I_c(i, j) = \frac{I_b(i, j)}{A(0)} \tag{3}$$

where $I_b(i,j)$ and $I_c(i,j)$ refer to the baseline corrected and the zero-conversion scaled intensity at wavelength j for spectrum i, respectively, and $A(0)$ refers to the area under the carbonyl peak at zero conversion. Figure 14 shows the predicted versus measured plots using this PLSR model, whereas Table V shows the standard deviations in the BA concentration for both methods. These results show that this PLSR gives reasonable predictions for the BA concentration, although the accuracy is lower than those obtained in the univariate experiments, whereas the precision is approximately the same. The reason for this may be twofold: in the calibration set, a homopolymerization was used, whereas the predicted values are from a copolymerization. The overall carbonyl band is the result of the carbonyl contributions from both monomer and (co)polymer, and as a result of a different copolymer composition, the shape of the CO band may change slightly. Another reason may be, as mentioned before, a difference in experimental or instrumental conditions.

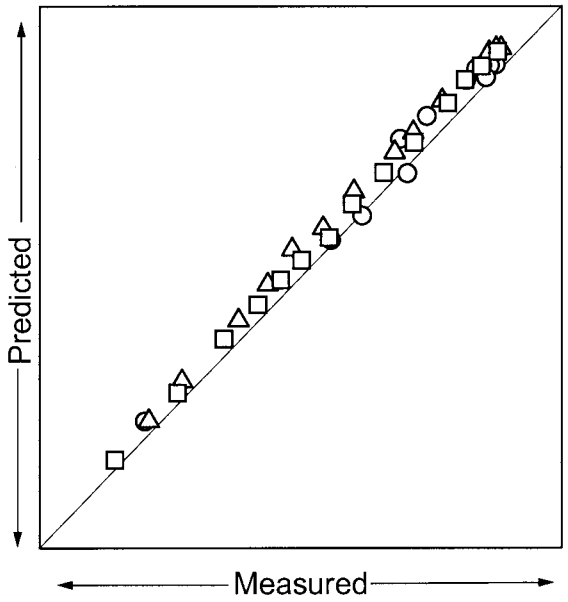

Figure 14 Predicted concentration of BA versus measured concentration of BA using results from B2 for calibration. ○, C1; △, C2; □, C3.

Thus, a simple answer cannot be given to the question whether the multivariate technique is preferred over the univariate technique. If considerable variation in the instrument and/or experimental conditions is anticipated, the univariate approach may be the method of choice. However, if instrumental variation is small, and experimental conditions are well within defined limits, the multivariate approach is preferred.

CONCLUSIONS

The copolymerization of styrene and butyl acrylate in dioxane was monitored by on-line Raman spectroscopy. It was shown that both univariate and multivariate techniques can be used for an accurate prediction of the monomer concentrations. After normalizing to a solvent peak, single factor models are obtained in PLSR. In principle, the multivariate approach gives the highest pre-

cision. The univariate method, on the other hand, gives more robust models, which can be used in a wide(r) range of monomer concentrations. Both PCA and PLSR indicate that the accuracy of PLSR is limited by the instrumental variation. In this work, only simple data preprocessing techniques have been applied to improve the robustness of the model. Nevertheless, univariate as well as multivariate approaches can be applied successfully in the calculation of monomer concentrations during copolymerization reactions, offering possibilities for on-line control of copolymerization reactions using Raman spectroscopy as the instrument for obtaining monomer concentrations.

The authors thank Han Witjes for valuable comments and discussion. The Foundation Emulsion Polymerization (SEP) and Priority Program Materials (PPM-NWO) are acknowledged for financial support.

REFERENCES

1. Schoonbrood, H. A. S.; Brouns, H. M. G.; Thijssen, H. A.; van Herk, A. M.; German, A. L. Macromol Symp 1995, 92, 133–156.
2. Mayo, F. R.; Lewis, F. M. J Am Chem Soc 1944, 66, 1594.
3. Guyot, A.; Guillot, J.; Rios Guerrero, L. In Emulsion Polymers and Emulsion Polymerizations; Bassett, D. R.; Hamielec, A. E., Eds.; ACS Symp Ser, 1981; Vol. 165; pp. 415–436.
4. Gossen, P. D.; MacGregor, J. F.; Pelton, R. H. Appl Spectrosc 1993, 47, 1852–1870.
5. Wu, C.; Danielson, J. D. S.; Callis, J. B.; Eaton, M.; Ricker, N. L. Process Contr Qual 1996, 8, 1–23.
6. Schork, F. J.; Ray, W. H. In Emulsion Polymers and Emulsion Polymerizations; Bassett, D. R.; Hamielec, A. E., Eds.; ACS Symp Ser, 1981; Vol. 165; pp. 505–514.
7. Siani, A.; Apostolo, M.; Morbidelli, M. In 5th Internation Workshop on Polymer Reaction Engineering; Reichert, K.-H.; Moritz, H.-U., Eds.; DECHEMA Monographs, VCH: Frankfurt, 1995; Vol. 131; pp. 149–157.
8. Moritz, H.-U. In Polymer Reaction Engineering; Reichert, K.-H.; Geiseler, W., Eds., VCH: Weinheim, 1989; pp. 248–265.
9. Morbidelli, M.; Storti, G. In Polymeric Dispersions: Principles and Applications; Asua, J. M., Ed.; Kluwer Academic Publishers: Dordrecht, 1997; pp. 349–361.
10. Gulari, E.; McKeigue, K.; Ng, K. Y. S. Macromolecules 1984, 17, 1822–1825.
11. Damoun, S.; Papin, R.; Ripault, G.; Rousseau, M.; Rabadeux, J. C.; Durand, D. J Raman Spectrosc 1992, 23, 385–389.
12. Hergeth, W.-D. In Polymeric Dispersions: Principles and Applications; Asua, J. M., Ed.; Kluwer Academic Publishers: Dordrecht, 1997, pp. 243–256.
13. Wang, C.; Vickers, T. J.; Schlenoff, J. B.; Mann, C. K. Appl Spectrosc 1992, 46, 1729–1731.
14. Wang, C.; Vickers, T. J.; Mann, C. K. Appl Spectrosc 1993, 47, 928–932.
15. Claybourn, M.; Massey, T.; Highkock, J.; Gogna, D. J Raman Spectrosc 1994, 25, 123–129.
16. Dubois, E.; Amram, B.; Charmot, D.; Menardo, C.; Ridoux, J.-P. Proc SPIE-Int Soc Opt Eng 1995, 2089, 470–471.
17. Özpozan, T.; Schrader, B.; Keller, S. Spectrochim Acta Part A 1997, 53, 1–7.
18. Al-Khanbashi, A.; Hansen, M. G.; Wachter, E. A. Appl Spectrosc 1996, 50, 1086–1092.
19. Vickers, T. J.; Lombardi, D. R.; Sun, B.; Wang, H.; Mann, C. K. Appl Spectrosc 1997, 51, 1251–1253.
20. Adar, F.; Geiger, R.; Noonan, J. Appl Spectrosc Rev. 1997, 32, 45–101.
21. Bowley, H. J.; Biggin, I. S.; Gerrard, D. L. In Time-Resolved Vibrational Spectroscopy; Laubereau, A.; Stockburger, M., Eds.; Springer-Verlag: New York, 1986; pp. 194–195.
22. Haigh, J.; Brookes, A.; Hendra, P. J.; Strawn, A.; Nicholas, C.; Purbrick, M. Spectrochim Acta Part A 1997, 53, 9–19.
23. Al-Khanbashi, A.; Dhamdhere, A. M.; Hansen, M. G. Appl Spectrosc Rev 1998, 33, 115–130.
24. Jawhari, T.; Hendra, P. J.; Willis, H. A.; Judkins, M. Spectrochim Acta Part A 1990, 46, 161–170.
25. Chu, B.; Fytas, G.; Zalczer, G. Macromolecules 1981, 14, 395–397.
26. Ellis, G.; Claybourn, M.; Richards, S. E. Spectrochim Acta Part A 1990, 46, 227–241.
27. Martens, H.; Næs, T. Multivariate Calibration; John Wiley & Sons, Ltd.: Chichester, 1989.
28. Baranska, H.; Labudzinska, A.; Terpenski, J. Laser Raman Spectrometry: Analytical Applications; Majer, J. R., Transl.; Ellis Horwood: Chichester, 1987; p. 87.
29. van den Brink, M.; van Herk, A. M.; German, A. L. J Polym Sci Part A Polym Chem, to appear.
30. Witjes, H.; Melssen, J. W.; In 't Zandt, J. J. A.; van der Graaf, M.; Heerschap, A.; Buydens, L. C. M., to appear.
31. The Unscrambler, software manual, Camo AS, 1996; pp. 325–327.